Study of Low Frequency Magnetic Shielding of a Thin Al/Steel/Al Composite in Various Applications

Paul Clérico, Xavier Mininger, Laurent Prevond, Thierry Baudin, Anne-Laure Helbert

Study of Low Frequency Magnetic Shielding of a Thin Al/Steel/Al Composite in Various Applications

P. Clérico[1,2,3], X. Mininger[2], L. Prévond[3], T. Baudin[1], A-L. Helbert[1]

[1]ICMMO, SP2M, Univ. Paris-Sud, Université Paris-Saclay, UMR CNRS 8182, Orsay, France

[2]GeePs, CentraleSupélec, Univ. Paris-Sud, Université Paris-Saclay, Sorbonne Université, UMR CNRS 8507, Gif-sur-Yvette, France

[3]SATIE-Cnam, ENS Paris Saclay, Univ. Paris-Sud, UMR CNRS 8029, Cachan, France

***Abstract*—A composite constituted of a steel sheet taken in a sandwich between two aluminum (Al) sheets is produced by cold roll bonding. A good adherence between Al and steel sheets, ensuring a good mechanical resistance, is obtained with a specific process. A previous work of the authors has shown that optimal condition between adherence and magnetic shielding effectiveness (SE_H) is obtained with a 230 µm composite produced with an initial thickness of Al and steel sheets respectively of 250 and 100 µm. In this paper, the 230 µm Al/Steel/Al composite is used in three applications modelized by 2D numerical simulations. To facilitate calculations, a homogenization method is applied to the composite. Studied applications are a cylindrical box containing a coil, a square box under an external magnetic field and a high voltage cable. In each application, SE_H is calculated at low frequency (1 Hz – 100 kHz) and different materials (Al/Steel/Al, Al, steel, and copper) are compared. It is observed that, in each application, the composite is more advantageous at equal mass and especially at frequencies higher than around 5-10 kHz.**

***Index Terms*—Cold Roll Bonding, Finite Element Method, Homogenization, Shielding Effectiveness**

I. Introduction

Electromagnetic pollution is a source of disturbance to sensitive electrical and electronic devices [1] and can be potentially harmful to human beings [2]. Living and critical components must be then protected from electric and magnetic fields, and electronic devices must confine them thanks to electromagnetic shielding [3, 4]

Common materials used for electromagnetic shields are metals [5, 6] and carbons [7, 8]. Lightweight materials, required in the transportation industry, composed of metal or carbon reinforced polymer have been greatly studied [9, 10]. However, polymers are insulating, and reinforced polymer composites show lower electrical conductivity than metal bulk. Multilayer composite is also an effective means to shield against electromagnetic fields [11, 12].

Low frequency magnetic fields can cause noise and disturbance to sensitive devices and are emitted, for example, by motors, power supplies, and switches. In this paper, the shielding effectiveness (SE_H) of a 230 µm Al/Steel/Al composite with homogenized properties is studied and compared to Al, steel, and copper ones in various applications modelized by the finite element method (FEM). The idea is to propose a solution that gives an efficient shielding effectiveness against both static and low frequency electromagnetic fields. Furthermore, the thin composite thickness allows ensuring its lightness and flexibility. Another main interesting advantage of this solution is that Al layers in the composite protect the steel layer from potential oxidation. Thus, the composite presents the advantage of being adapted to oxidizing atmospheres. Consequently, SE_H is studied in this paper for a magnetic field at low frequencies from 1 Hz to 100 kHz. Both experimental and numerical approaches, including homogenization process, are used to present the global study, from the elaboration of the composite material to the shielding application.

II. Materials and applications

A. Al/Steel/Al composite

The studied composite is composed of one layer of steel sandwiched between two layers of aluminum (Al). Commercial low carbon steel DC01 and 8011-aluminum alloy are chosen as raw materials with a respectively initial thickness of 100 µm and 250 µm.

DC01 steel is mainly used for drawing and forming applications. 8011-Al is a Fe and Si based aluminum alloy which is widely used in the industry. The chemical compositions of these two materials are listed in Table 1.

The Al/Steel/Al composite is produced by cold roll bonding (CRB) with different reduction rate (h_f / h_i). Figure 1 presents a schematic diagram of the composite CRB following rolling-normal cross-section (RD-ND).

TABLE 1
CHEMICAL COMPOSITIONS (%WT.) OF DC01 STEEL AND 8011-AL ALLOY

Al8011								
%Al	%Fe	%Si	%Mn	%Zn	%Cu	%Ti	%Cr	%Mg
Bal.	0.6 - 1	0.5 - 0.9	≤ 0.2	≤ 0.1	≤ 0.1	≤ 0.08	≤ 0.05	≤ 0.05
DC01								
	%Fe	%C	%Mn	%P	%S	%Si	%Al	
	Bal.	≤ 0.12	≤ 0.6	≤ 0.045	≤ 0.045	≤ 0.03	≤ 0.02	

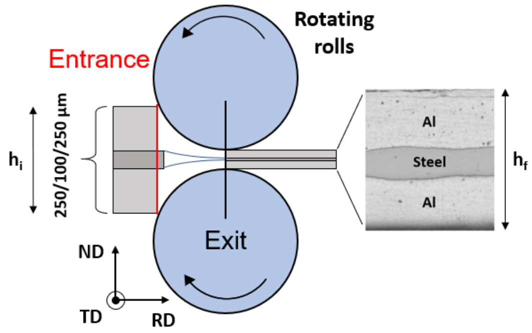

Figure 1: Cold roll bonding of Al/Steel/Al composite

In a previous study [13], the trade-off between shielding effectiveness and Al/Steel interfaces adherence has been studied. The following part proposes a summary that justifies the later thickness of the composite used for our applications.

Figure 2 shows the electronic assembly used to measure the experimental shielding effectiveness of the composite. A sinusoidal current is produced by a low-frequency generator associated with a linear amplifier. The effective intensity of this current is 2 A. A coil with a height of 18.5 mm, an inner and outer diameter of 15 and 30 mm generates a magnetic field. This magnetic field is then measured by a Hall effect sensor with a sensibility of 5.0 ± 0.1 mV/G. A cooling fan is employed to limit the temperature influence.

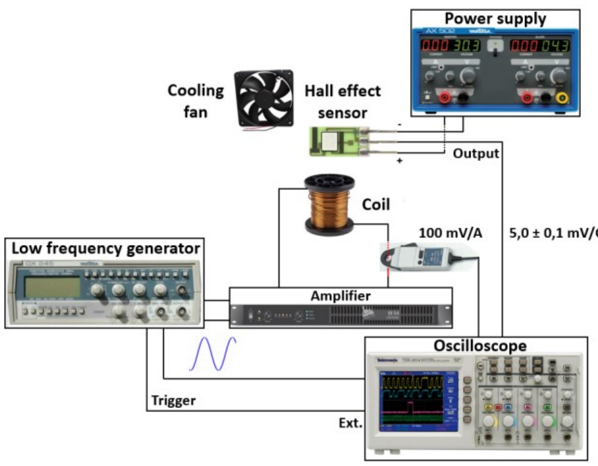

Figure 2: Electronic assembly scheme

Figure 3 shows that the experimental shielding effectiveness of 3 x 3 cm² samples measured at 1 Hz and 10 kHz decreases firstly linearly due to the thickness reduction, and then continues to decrease with a steeper slope due to the steel fragmentation that occurred during the CRB.

Figure 4 shows that the quality of Al/Steel interface adherence increases with the reduction rate. Adherence has been determined by tensile bond strength test (TBST) and the mean value has been calculated for each reduction rate. This method is detailed in a previous paper [13].

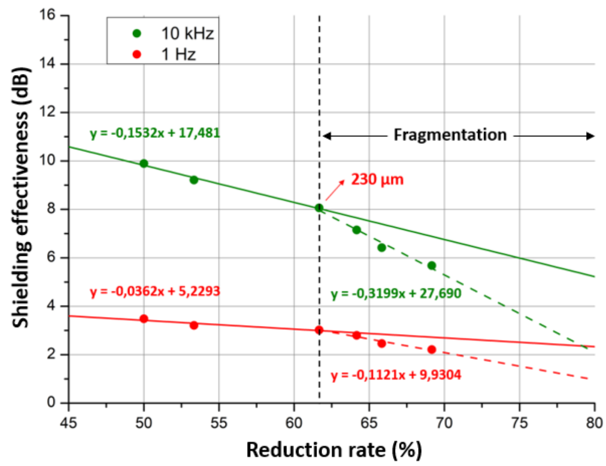

Figure 3: Shielding effectiveness of 3 x 3 cm² tri-layer samples at different reduction rate measured experimentally [13]

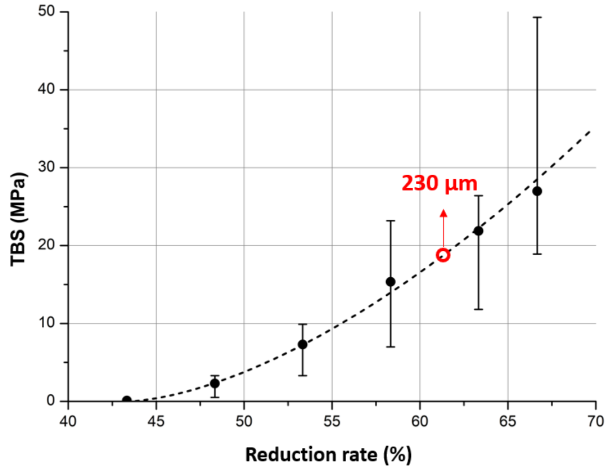

Figure 4: Tensile Bond Strength (TBS) of Al/Steel interfaces [13]

The optimal condition between shielding effectiveness and adherence of Al/Steel interfaces is then obtained with a 230 µm thickness composite. Indeed, the 230 µm composite shows very little steel fractures, that limit the negative effect on shielding effectiveness, and attain a good quality of adherence with a tensile bond strength around 19-20 MPa. In this case, aluminum and steel layer thicknesses of the composite considered in the numerical approach are then around 191.6 (2 × 95.8) and 38.4 µm.

B. Applications

In this paper, three applications are modelized in Comsol Multiphysics with AC/DC module and studied in the range of [1 Hz – 100 kHz]: a cylindrical box containing a coil to simulate the confinement of a magnetic field, a squared box placed in an external magnetic field to simulate the protection of a sensitive component and finally a simplified model of a high voltage cable that is closer to actual industrial applications. Figures 5, 6 and 7 show the modelized geometry of the three applications.

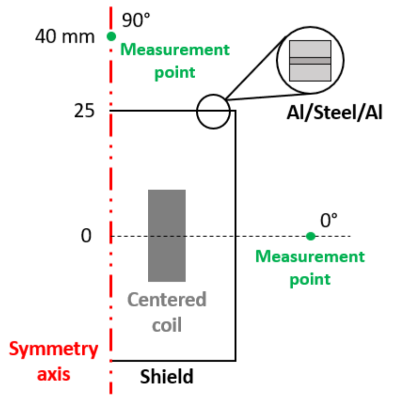

Figure 5: Cylindrical shielding box (50 x 50 mm) containing a coil (2D-axi). SE_H measurement points are indicated

The cylindrical box is modelized with a 2D axisymmetric model. The box has a diameter and a height of 50 mm. In this first approach, the coil is considered centered inside the cylindrical box. To simulate the magnetic field, an effective current of 2 A, corresponding to a current density of around 1.44e6 A/m², is considered. The shielding effectiveness of this box is studied at two points, one horizontal and one vertical, both situated at 15 mm of the shield. This first application allows simulating the magnetic shielding with a near-field condition.

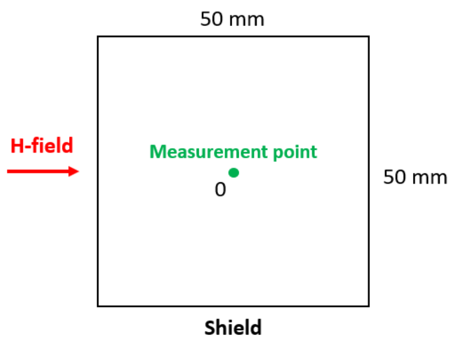

Figure 6: Square shielding box (50 x 50 mm) under an external H-field (2D). SE_H measurement point is located at the box center

The squared box is modelized with a 2D plane model. The box has a side of 50 mm and is placed in an external magnetic field obtained with magnetic vector boundaries condition ($n \times A = n \times A_0$). The shielding effectiveness is studied at the center of the box. This second application allows simulating the magnetic shielding with a far-field condition.

The high voltage cable is also modelized with a 2D plane model. The simplified modelized geometry (Figure 7) has been inspired by the work of [14]. Figure 8 shows the actual geometry of the high voltage cable studied by [14]. In a high voltage cable, perturbations can take place affecting cable integrity and leading to malfunctions. A correct shielding can prevent these perturbations.

The total diameter of the cable is 78 mm. The cable has four copper wires with a diameter of 16.4 mm. The current density running through the copper wires is equal to 1e6 A/m² and is defined positively in two wires and negatively in the two others. A shield surrounds each wire to limit proximity effects, and another one surrounds the four wires for a global shielding of the cable. The area, other than copper and shield, is considered as PET (polyethylene terephthalate). The shielding effectiveness is studied at 1 cm from the high voltage cable.

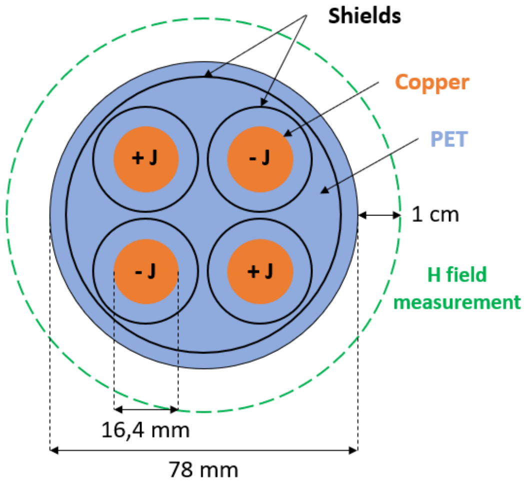

Figure 7: Simplified model of a high voltage cable (2D). SE_H measurement line is at 1 cm away from the cable

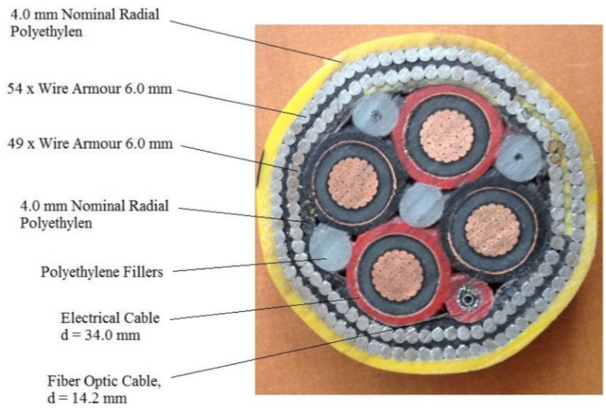

Figure 8: Example of an actual high voltage cable with four copper wires [14]

In each application, the following equations are resolved:

$$\nabla \times H = J \tag{1}$$

$$B = \nabla \times A \tag{2}$$

$$E = -j\omega A \tag{3}$$

$$J = \sigma E + J_e \tag{4}$$

with H the magnetic field, B the magnetic induction, A the magnetic vector potential, E the electrical field, J the total current density, J_e the external current density, σ the electrical conductivity, and ω the angular frequency.

For the near-field application and the high voltage cable, the modelized system is bounded by a layer of infinite elements.

The magnetic shielding effectiveness (SE_H) is defined by:

$$SE_H = 20\log_{10}\frac{H_0}{H_{shield}} \quad (5)$$

with H_0 and H_{shield} respectively the magnetic field without and with the shield at the different measurement points defined previously. SE_H is studied in each application at low frequencies from 1 Hz to 100 kHz.

The use of the 230 µm Al/Steel/Al composite in these applications is compared to aluminum (Al), steel, and copper (Cu) in two cases: first with equal thickness for applications with low space available, and then with equal mass especially adapted for embedded applications. The following densities are used for calculations: 2.71 for Al, 8.96 for Cu, 7.85 for steel and 3.57 g/cm^3 for the composite. Thus, the 230 µm Al/Steel/Al composite is 2.5 and 2.2 times less dense than Cu and steel, but 1.3 times denser than Al.

Materials properties considered into the numerical model for the magnetic shielding are summed up in Table 2.

TABLE 2
RELATIVE PERMEABILITY AND CONDUCTIVITY OF CU, AL AND STEEL

Material	Relative permeability µ	Conductivity σ, 10^6 S/m
Cu	1	59.98
Al	1	33.61
Steel	250	9.02

The numerical modeling of actual devices with the consideration of the heterogeneous layers of the composite is a real challenge regarding the scale differences from the material to the application. As a consequence, the composite material properties are here homogenized to give reasonable computation time for the simulations. The principle of homogenization is shown in Figure 9. The properties of an equivalent layer are determined in order to obtain the same shielding effectiveness of the tri-layer composite.

In the case of the 230 µm composite, the determined equivalent properties are resumed in Table 3. A slight difference is observed between RD and TD properties. The presence of a few steel fractures considered in the homogenization process explains this difference. More details of the method to determine these properties by an energy approach can be found in our previous paper [13].

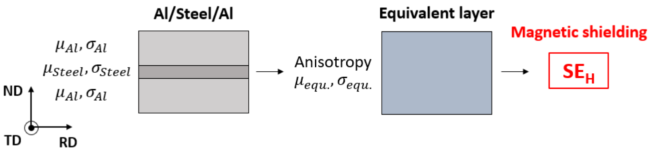

Figure 9: Homogenization principle of the tri-layer composite

TABLE 3
EQUIVALENT RELATIVE PERMEABILITY AND EQUIVALENT CONDUCTIVITY OF A 230 µM AL/STEEL/AL COMPOSITE

Direction	Relative permeability µ	Conductivity σ, 10^6 S/m
Rolling direction (RD)	41.61	29.507
Transverse direction (TD)	42.40	29.511
Normal direction (ND)	1.20	23.140

III. RESULTS AND DISCUSSION

A. *Homogenization validation*

Before comparing the shielding effectiveness of the composite with Al, Cu and steel, homogenization method has to be validated by comparing the shielding effectiveness of the equivalent layer with the tri-layer one.

The comparison between the tri-layer and the equivalent layer is shown in Figure 10 for the cylindrical box with the measurement of the magnetic field at the vertical point.

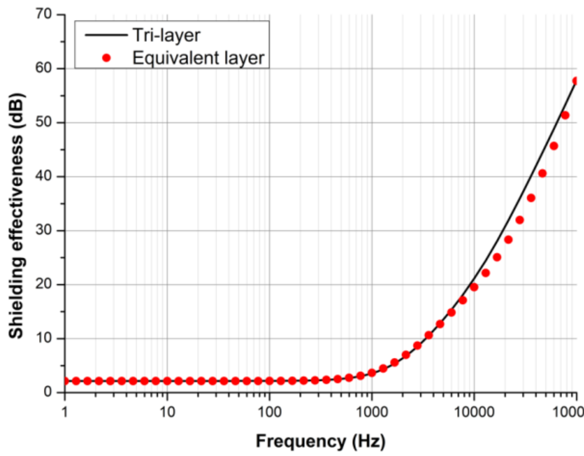

Figure 10: Shielding effectiveness of the tri-layer Al/Steel/Al and its equivalent layer in the cylindrical box application (vertical point)

It is observed that the equivalent layer, with its properties determined by homogenization, has an excellent concordance with the tri-layer.

However, a slight difference can be seen for frequencies higher than 5 kHz. Indeed, the equivalent layer shows shielding effectiveness lower than the tri-layer with a maximal difference around 4 dB.

One parameter linked to the shielding effectiveness at high frequencies is the skin depth [15]. Table 4 gives the skin depth of Al, steel and the equivalent layer at different frequencies.

TABLE 4
SKIN DEPTH AT DIFFERENT FREQUENCIES IN AL, STEEL AND THE EQUIVALENT LAYER

Frequency (Hz)	Skin depth (µm)		
	Al	Steel	Equivalent layer
1	86 813	10 598	14 296
1 000	2 745	335	452
10 000	868	106	143
100 000	274	33.5	45.2

As a reminder, the Al layer and steel layer thicknesses are respectively around 95.8 and 38.4 µm. Figure 11 shows the layer thickness divided by the skin depth in function of frequency for Al, steel and the equivalent layer.

The skin depth in Al is thicker than the layer thickness for all frequencies, then the magnetic field is very little absorbed by Al. The skin depth in steel attains the layer thickness at around 77 kHz. By definition [15], around 63 % of the magnetic field is then absorbed by steel at 77 kHz. The skin depth attains the equivalent layer thickness at around 4 kHz. Thus, the equivalent layer absorbs better the magnetic field than the tri-layer composite. This difference in skin depth could explain the slight difference in shielding effectiveness at a frequency higher than 5 kHz.

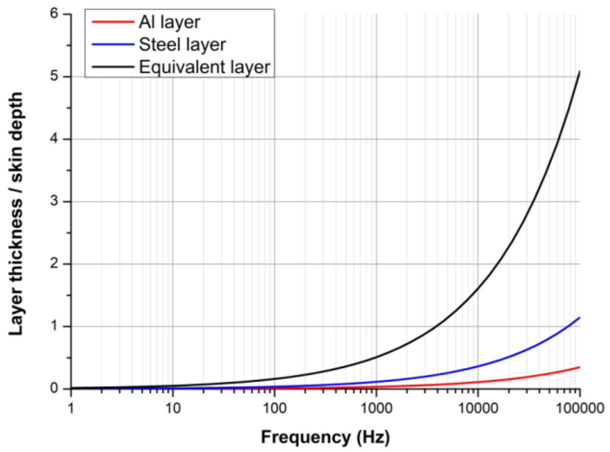

Figure 11: Layer thickness divided by the skin depth for Al, steel and the equivalent layer

B. Applications

The shielding effectiveness of the cylindrical box measured at the vertical and horizontal points are respectively presented in Figures 12 and 13. SE_H is calculated with shields at equal thickness and at equal mass. The results at these different points are sensibly similar. The shielding effectiveness is, nevertheless, a little higher at the vertical point than at the horizontal one.

As expected, copper and aluminum do not shield low frequencies under 500 Hz due to their low relative permeability (close to 1). At higher frequencies, Cu shows better shielding effectiveness than Al with equal thickness due to its higher conductivity.

Steel can shield low frequencies thanks to its high relative permeability. Furthermore, its increase in higher frequencies is steeper than Cu and Al. This steeper slope could be explained by a thinner skin depth in steel than in Cu and Al for a given frequency. Moreover, it can be noticed that the increase of shielding effectiveness of steel begins at a higher frequency (≈ 2 kHz) than for Cu or Al (≈ 500 Hz) due to its smaller conductivity.

The homogenized composite can also shield low frequencies with a shielding effectiveness a little lower than the steel one due to its lower relative permeability. In the equal thickness study, the shielding effectiveness of the composite is lower than the steel one on the entire frequency range. The use of the composite is then more advantageous at equal mass, its shielding effectiveness is greater than other ones at frequencies higher than 2 kHz.

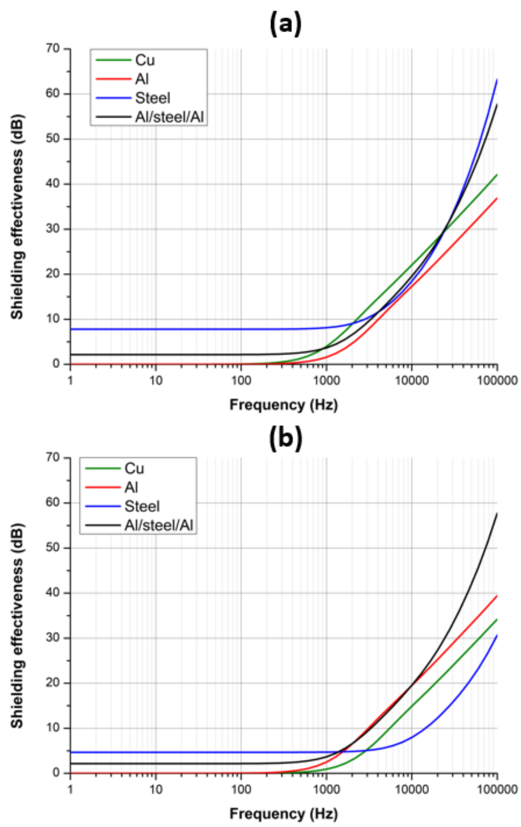

Figure 12: Shielding effectiveness of the cylindrical box with equal thickness (a) and equal mass (b) measured at the **vertical point**

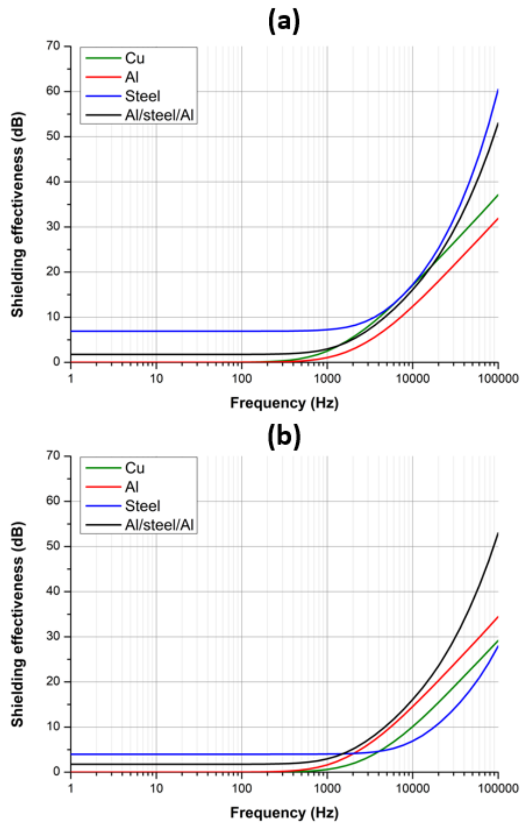

Figure 13: Shielding effectiveness of the cylindrical box with equal thickness (a) and equal mass (b) measured at the **horizontal point**

Figures 14 and 15 introduce respectively the results of the equal thickness and equal mass studies for the squared box and the high voltage cable.

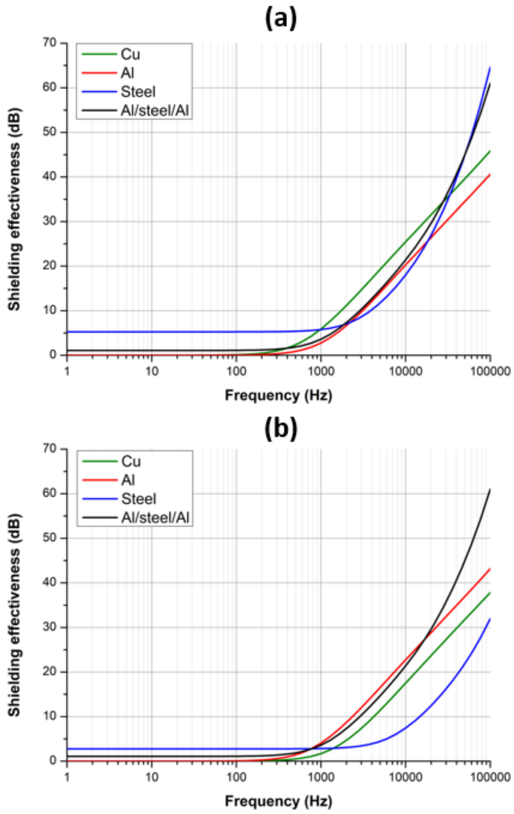

Figure 14: Shielding effectiveness of the squared box with equal thickness (a) and equal mass (b) measured at the **central point**

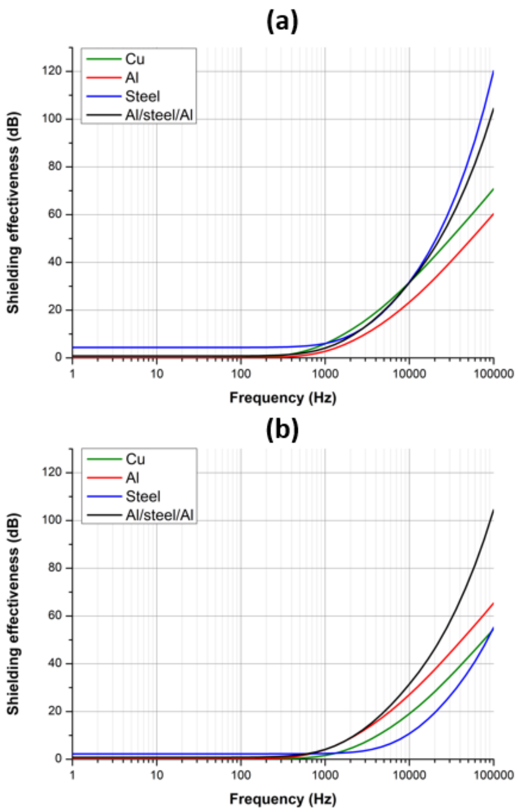

Figure 15: Shielding effectiveness of the high voltage cable with equal thickness (a) and equal mass (b) measured at **1 cm** away from the cable

The curves obtained are very similar to the cylindrical box ones. As previously, it is observed that the Al/Steel/Al composite is more advantageous at equal mass and at frequencies higher than 2 – 10 kHz.

The composite could be still interesting at equal thickness. Indeed, its shielding effectiveness at high frequency is near to the steel one and can be higher than the Cu one with a lower density.

To give some quantitative comparisons, Figure 16 resumes the results of the equal mass study for the three applications. The shielding effectiveness at 1 Hz, 1, 10 and 100 kHz are drawn for the four studied materials. Cu has a shielding effectiveness a little bit lower than Al due to its higher density. Indeed, SE_H of Cu and Al at 100 kHz is respectively around 37.8 and 43.2 dB in the far-field application and 34.2 and 39.4 dB in the near-field application. Steel is able to shield low frequencies (< 1 kHz) but has a lower shielding effectiveness at high frequency than Cu and Al: at 1 Hz and 100 kHz, respectively 2.7 and 32 dB in the far-field application, and 4.7 and 30.7 dB in the near-field application.

The shielding effectiveness attained with the high voltage cable is greater than with the two previous applications: at 100 kHz, SE_H of Cu, Al, steel, and the composite is respectively 54.5, 65.4, 55.2, and 104.5 dB. The presence of several shields, around each wire, and around the four wires, explains this difference.

It is observed that for each application, the homogenized composite is an interesting compromise at equal mass to shield low frequency (< 1 kHz) and high frequency (> 10 kHz). In the case of the cylindrical box (near-field application), its shielding effectiveness at 1 Hz is around 2.1 dB, lower than the steel one, but better than the Cu and Al ones that do not shield very low frequencies. At 100 kHz, its shielding effectiveness is around 57.7 dB, better than Cu, Al and steel ones.

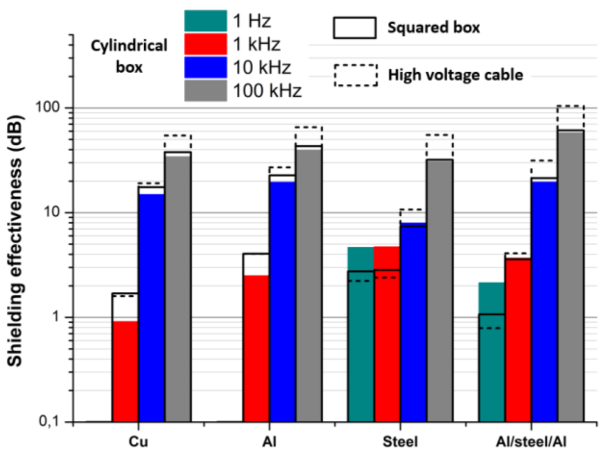

Figure 16: Shielding effectiveness of the cylindrical box, the squared box and the high voltage cable with different materials and frequencies at equal mass

IV. Conclusion

A composite constituted of a steel sheet sandwiched between two aluminum (Al) sheets has been successfully elaborated by cold roll bonding. The optimal condition between magnetic shielding and Al/Steel interface adherence is attained with a tri-layer composite of 230 µm. The homogenization method used to determinate the material properties of an equivalent layer of this composite has been validated by the great concordance between the shielding effectiveness of the equivalent layer and the tri-layer one.

The shielding effectiveness of the 230 µm Al/Steel/Al composite has then been studied in three applications with numerical simulation and compared to individual Cu, Al, and steel layers. It has been shown that the Al/Steel/Al composite is more advantageous at equal mass in each application. Indeed, the tri-layer composite is able to shield very low frequency (< 1 kHz) and has shielding effectiveness at high frequency (> 10 kHz) greater than Cu, Al, and steel. Its shielding effectiveness at 1 Hz varies in function of the modelized application between 0.8 and 2.1 dB compared to the steel one that varies between 2.2 and 4.7 dB. At 100 kHz, it varies between 57.7 and 104.5 dB compared to the Cu, Al, and steel ones that vary respectively between 34.2 and 54.5, 39.4 and 65.4, and 30.7 and 55.2 dB.

Thereby, the study of the shielding effectiveness of the composite with more complex and realist geometry could be interesting. The equivalent layer with homogenized properties can be used in 3D models to reduce calculation and CPU time. This work can be extended to other materials in order to increase the shielding effectiveness, especially at low frequency with a higher relative permeability material.

References

[1] R. Smolenski, J. Bojarski, A. Kempski, and P. Lezynski, "Time-domain-based assessment of data transmission error probability in smart grids with electromagnetic interference", *IEEE Trans. Ind. Electron*, vol. 61, pp. 1882-1890, 2014

[2] T.W. Dawson, K. Caputa, M.A. Stuchly, R.B. Sphaphard, R. Kavet, and A. Sastre, "Pacemaker interference by magnetic fields at power line frequencies", *IEEE Trans. Biomed. Eng.*, vol. 49, pp. 254-262, 2002

[3] W. Abdelli, X. Mininger, L. Pichon, H. Trabelsi, Impact of composite materials on the shielding effectiveness of enclosures, Applied Computational Electromagnetics Society Journal, vol. 27 (4), pp. 369–375, 2012

[4] S. Ahn *et al.*, "Low frequency electromagnetic field reduction techniques for the On-Line Electric Vehicle (OLEV)," *2010 IEEE International Symposium on Electromagnetic Compatibility*, pp. 625-630, 2010

[5] X. Liu, J. Wu, J. He, L. Zhang, Electromagnetic interference shielding effectiveness of titanium carbide sheets, Materials Letters, vol. 205, pp. 261–263, 2017

[6] Z. Xu, H. Hao, Electromagnetic interference shielding effectiveness of aluminum foams with different porosity, Journal of Alloys and Compounds, vol. 617, pp. 207-213, 2014

[7] D. D. L. Chung, Electromagnetic interference shielding effectiveness of carbon materials, Carbon, vol. 39 (2), pp. 279-285, 2001

[8] M. Z. Li, L. C. Jia, X. P. Zhang, D. X. Yan, Q. C. Zhang, Z. M. Li, Robust carbon nanotube foam for efficient electromagnetic interference shielding and microwave absorption, Journal of Colloid and Interface Science, vol. 530, pp. 113-119, 2018

[9] A. A. Al-Ghamdi, O. A. Al-Hartomy, F. El-Tantalwy, F. Yakuphanoglu, Novel polyvinyl alcohol/silver hybrid nanocomposites for high performance electromagnetic wave shielding effectiveness, Microsyst Technol, vol. 21 (4), pp. 859-868, 2015

[10] M. Ray, J. J. George, A. Chakraborty, A. K. Bhowmick, An investigation of the electromagnetic shielding effectiveness of ethylene vinyl acetate elastomer reinforced with carbon nanofillers, Polym. Compos., vol. 18, pp. 59-65, 2010

[11] X. Ma, Q. Zhang, Z. Luo, X. Lin, G. Wu, A novel structure of Ferro-Aluminum based sandwich composite for magnetic and electromagnetic interference shielding, Materials and Design, vol. 89, pp.71-77, 2016

[12] D. H. Kim, Y. Kim, J. W. Kim, Transparent and flexible film for shielding electromagnetic interference, Materials and Design, vol. 89, pp. 703-707, 2016

[13] P. Clérico, X. Mininger, L. Prévond, T. Baudin, A-L. Helbert, Compromise between magnetic shielding and mechanical strength of thin Al/Steel/Al sandwiches produced by cold roll bonding: experimental and numerical approaches, Journal of Alloys and Compounds, vol. 798, pp. 67-81, 2019

[14] Duc Quang Nguyen, Développement d'un outil d'investigation pour le diagnostic des phénomènes hautes fréquences dans les câbles électriques, PhD thesis, École Nationale Supérieure d'Arts et Métiers, 2013

[15] Schelkunoff, S.A., Electromagnetic Waves, Bell Telephone Laboratories series, Van Nostrand, 1943